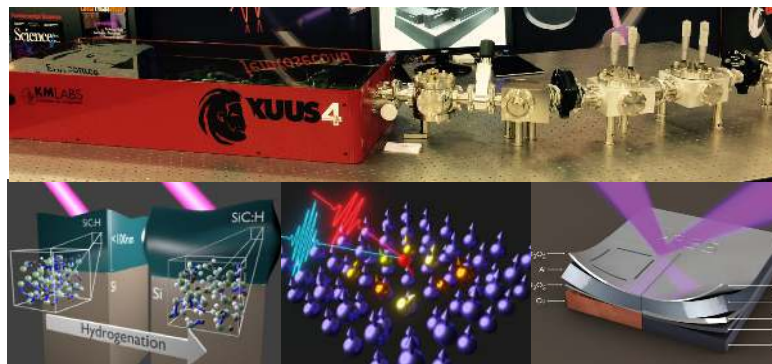


# Ultrafast Coherent EUV beams using the KMLabs Wyvern and XUUS<sub>4</sub><sup>TM</sup>



Xiaoshi Zhang, Eric Mountford, Matthew Kirchner, and Henry Kapteyn  
KMLabs, Inc., Boulder CO

The KMLabs Wyvern ultrafast amplifier, combined with the KMLabs XUUS<sub>4</sub><sup>TM</sup> high-harmonic-generation source system, provides the 1st ultra-stable, engineered, coherent EUV beams, at flux levels enabling a broad range of applications in spectroscopy and imaging – including at the technologically significant EUV lithography wavelength of 13.5nm ( $\approx 92\text{eV}$ ).



## 1. Introduction

Just as the invention of the visible laser revolutionized science and technology, the recent development of commercial tabletop-scale laser sources at *much shorter wavelengths* - in the EUV and soft X-ray regions - will also have a transformative impact on nano and materials science and technology. The KMLabs XUUS<sup>TM</sup> EUV source is based on high-order harmonic generation (HHG), in which an intense high peak-power ultrafast laser is coherently and efficiently upshifted to higher photon energies using extreme nonlinear optics.<sup>[1]</sup> When properly phase-matched, the output HHG beams are highly spatially and temporally coherent, and perfectly synchronized to the driving laser, making them ideal for capturing the fastest nanoscale dynamics in material, nano, molecular and atomic systems. Indeed, KMLabs HHG sources have been used for many record-breaking achievements, including the highest spatial resolution imaging at the 13.5nm EUV lithography wavelength,<sup>[2,3]</sup> as well as capturing the fastest charge, spin and atomic motions in molecular,<sup>[4]</sup> magnetic,<sup>[5,6]</sup> material,<sup>[7]</sup> and nano systems.<sup>[8,9]</sup> Moreover, depending on the application, the HHG output can be tailored to obtain high femtosecond-to-attosecond time resolution, or high energy/spectral resolution (30 meV/0.1 nm).<sup>[10-15]</sup>

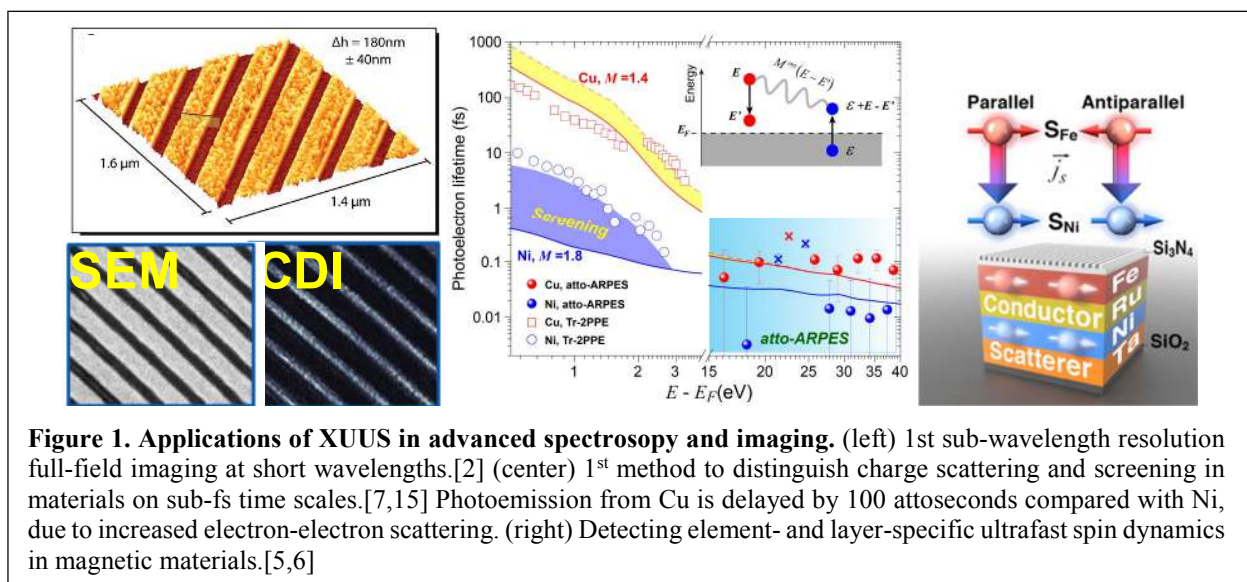
High harmonics are generated in the  $\approx 10$  fs timescale during which an atom in a gas undergoes field ionization by an intense femtosecond laser. However, optimally implementing an HHG source is not simply a matter of focusing laser light into a gas jet or cell. The emission from each individual atom has a broad dipole radiation distribution – to generate a bright HHG beam, the emission from many atoms must add coherently, in a process called phase matching. Phase matching ensures the highest efficiency, the best beam quality and the best control over the HHG spectrum – in close analogy with traditional nonlinear optics. In many experiments, if the objective

is to simply *observe* high harmonics, optimization of phase matching is not critical. In contrast, for more challenging real-world applications such as imaging, achieving high HHG flux is critical for success or for dynamic imaging.

In the past, scientists often needed to spend 1-3 years constructing and implementing a HHG source. Even then, the HHG stability and flux were often not optimized, requiring large lasers and setups with multiple vacuum pumps, leading to instability and often preventing the best success in a desired application.

KMLabs XUUS<sub>4</sub><sup>TM</sup> maximizes the conversion efficiency of laser-to HHG beams through phase-matched conversion in hollow waveguides.<sup>[16-19]</sup> Several key elements of a workhorse XUUS<sub>4</sub><sup>TM</sup> HHG “tabletop x-ray laser” system include:

- (1) An optimally-implemented, differentially-pumped, waveguide geometry for high-harmonic generation. This ensures optimal HHG phase matching, low gas load, and a compact setup for high stability.
- (2) A robust high average power, high repetition-rate, femtosecond laser that has been optimally designed and engineered for high HHG flux i.e. high average power, low pulse pedestal so that all the laser power is useful, optimized pulse duration, and high beam quality.
- (3) An EUV beamline delivery system engineered for excellent HHG intensity and wavefront stability, that are critical for most applications. This minimizes losses and manages thermal loading. This makes it possible to provide a stable, high-quality output beam for applications. KMLabs has supplied their XUUS<sub>4</sub><sup>TM</sup> system for several years as a fully integrated and specified system with their Dragon<sup>TM</sup> and Wyvern<sup>TM</sup> ultrafast laser systems.
- (4) Demonstrated ability to implement record sub-wavelength EUV imaging, as well as a host of attosecond-resolution EUV ARPES, MOKE, COLTRIMS and VMI spectroscopies.<sup>[2,4-15]</sup>



## 2. EUV Flux Test Overview

An example configuration used for HHG flux testing using a NIST-calibrated vacuum diode is shown in Figure 2. It consists of the KMLabs Wyvern, the KMLabs XUUS<sub>4</sub><sup>TM</sup>, and a modularized EUV imaging spectrometer beamline which is one of several of KMLabs' standard beamline configurations. Here we summarize the test results, and show that this configuration makes it possible to produce ultrastable EUV output in the photon energy range up to >100 eV (~10 nm) at flux levels that enable a broad set of scientific applications. The entire system, including the laser, the XUUS<sub>4</sub><sup>TM</sup>, and the beamline occupies a single modest-size optical table (~5'x10').

### 2.1 KMLabs Wyvern<sup>TM</sup>

The KMLabs Wyvern amplifier laser system is the only variable repetition rate amplifier in the high energy kHz-class market i.e. suitable for driving HHG. It's simple *single-stage* design makes it a cut above its closest competitors - that require more complex two-stage or dual-head architectures in order to reach similar power levels. Our patented cryogenic technology eliminates thermal lensing and heat management issues that limit the competition. The Wyvern design has been extensively tested for reliability and robust long-term operation.

### 2.2 KMLabs XUUS<sub>4</sub><sup>TM</sup>

The KMLabs XUUS<sub>4</sub><sup>TM</sup> is a highly-engineered HHG source and beamline system that allows users to generate coherent EUV light within a day of installation. The XUUS<sub>4</sub><sup>TM</sup> HHG source produces EUV light with optimal conversion efficiency, while the beamline modules dramatically simplify the delivery of the beam to the experiment with minimum loss, maximum flexibility and wide user customization. This approach lowers the entry barrier into this exciting area of coherent short wavelength science and technology.

KMLabs's XUUS<sub>4</sub><sup>TM</sup> system is built on a single rugged optomechanical platform. It takes a ~0.1-6 mJ energy, 1-100 kHz repetition-rate femtosecond (~20-40 fs) laser beam as the input and, depending on the XUUS<sub>4</sub><sup>TM</sup>

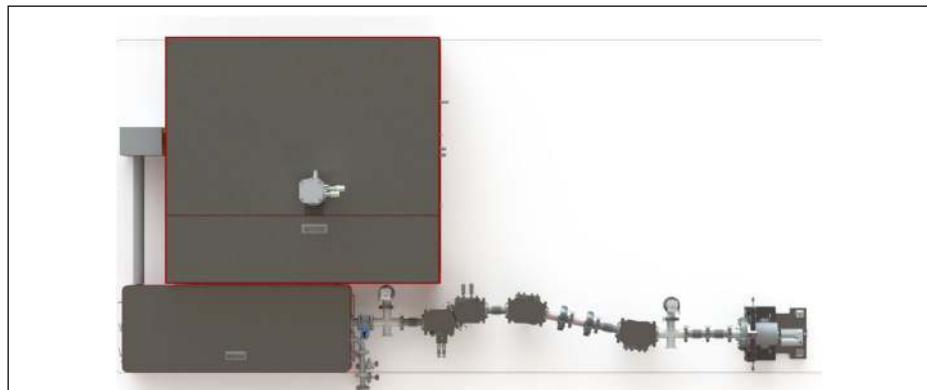


**Figure 2. XUUS/Wyvern system test configuration.** The laser beam output from a Wyvern amplifier is coupled into the KMLabs XUUS<sub>4</sub><sup>TM</sup>. A proprietary laser beam delivery system automatically aligns, stabilizes the pointing, focuses and couples the laser beam into the patented gas-filled hollow waveguide cartridge that minimizes gas usage and EUV absorption. The XUUS beamline components rejects the residual laser light, enabling robust background free and calibrated HHG flux measurement and spectral characterization. The entire system is controlled and measured using a fully-integrated XUUS<sub>4</sub><sup>TM</sup> control software and electronics.

configuration and drive laser parameters, produces bright coherent EUV beams (that can span into the soft x-ray beam region when driven by mid-IR or intense UV lasers). In the KMLabs

XUUS<sub>4</sub><sup>TM</sup>, the pump laser is focused into a gas-filled hollow waveguide<sup>[16-18]</sup> that maintains high intensity over an extended length. The XUUS<sub>4</sub><sup>TM</sup> incorporates a proprietary HHG waveguide cartridge design, as well as optimized differential pumping, to reduce gas usage to a minimum - allowing even expensive HHG gasses such as Ne, Kr and Xe to be used economically. Compared with a gas jet, the gas consumption is orders of magnitude less, and differential pumping allows for optimization of the target pressure while minimizing vacuum pump loading with any gas including Helium (which requires a high ~1 atm target pressure that cannot be effectively sustained using other configurations). Different gasses yield HHG spectra that are optimized for different spectral regions, with Xe/Kr ideal for longer wavelengths/lower photon energies, and He best suited for shorter wavelengths (i.e. 13.5 nm). Moreover, efficient differential pumping also avoids re-absorption of the generated HHG light.

Drive Laser Parameter	Value
<b>Pulse energy &amp; rep. rate:</b>	
• 30 nm HHG	0.5 mJ @ 10 kHz
• 13 nm HHG	3 mJ @ 3 kHz
<b>Center Wavelength</b>	790 nm
<b>Nanosecond Pulse contrast at full power</b>	500:1 Pre 100:1 Post
<b>Repetition Rate</b>	3 to 10 kHz
<b>Beam quality (M<sup>2</sup>)</b>	1.2 X, 1.2 Y
<b>Pulse Duration (measured by FROG)</b>	37 fs
<b>Beam Size (1/e<sup>2</sup> Diameter, 2<math>\omega</math>)</b>	10 mm
<b>Power stability</b>	<0.5% RMS for 8hrs

**Table 1:** Wyvern laser parameters used for the XUUS<sub>4</sub><sup>TM</sup> test.

Since the conversion efficiency of HHG depends strongly on the laser peak intensity (i.e. short pulse, tightly focusable beam with M<sup>2</sup>~1, minimal ASE), care is also taken to deliver the optimal beam to the waveguide. The XUUS’s proprietary laser beam management system maintains high positional, flux, intensity and wavefront stability of the HHG source over long-term operation (see Figs. 3 and 4). This is achieved by a computer-assisted automatic laser beam alignment and pointing stabilization system. It also includes a convenient real-time laser beam parameter monitoring and logging system. The result is that the pointing stability of the EUV source exceeds the pointing stability performance of the driving laser— a critical requirement for reliable alignment at EUV wavelengths. The excellent long-term and short-term stability results in the most stable and usable HHG source implemented to-date. This allows the user to treat the source as a true tabletop “x-ray laser,” rather than as an experiment in itself.

XUUS <sub>4</sub> <sup>TM</sup> Performance using Wyvern drive laser	Value
<b>Photon Flux at 30 nm (Argon) --at the source</b>	3.0 x10 <sup>12</sup> photons/sec/single harmonic
<b>Photon Flux at 13.5 nm (Helium) --at the source</b>	3.0x10 <sup>10</sup> photons/sec/single harmonic
<b>Spectral range</b>	10eV to 50eV (Argon) 25eV to 112eV (Helium)
<b>Beam Pointing stability</b>	<10 $\mu$ Rad for 8 hour
<b>Power stability</b>	<5 % RMS for 8 hour

**Table 2:** XUUS<sub>4</sub><sup>TM</sup> performance, pumped by the KMLabs Wyvern.

### 3. HHG Flux Test Results

We tested the XUUS/Wyvern HHG flux in two spectral regions:

- a) The “near-EUV” HHG spectrum generated in Argon gas with the spectrum peaked at ~42 eV (or ~35 nm wavelength); and
- b) The “deep EUV” spectrum generated in Helium gas, that peaks at ~92eV (at the technologically important 13.5 nm wavelength).

For the near-EUV region, the optimal pulse energy for highest HHG flux is 0.5 mJ, while for 13.5 nm, it is 3 mJ. It is important to note that the full energy of the Wyvern laser is not needed for EUV generation, so that a good portion of the output can be reserved for other purposes, such as pumping a frequency conversion step (e.g. SHG, OPA) for pump-probe experiments.

The measured key laser and EUV parameters are summarized in Tables 1 and 2. To obtain a quantitative measurement of the HHG flux, we used an EUV-sensitive CCD camera cross-referenced to a NIST-traceable EUV photodiode, along with beamline elements with previously-measured throughput. The beamline test configuration and calibration methodology are discussed in more detail in Appendix A.

The near and deep EUV spectra are shown in Figure 3, while the EUV beam power and pointing stability is shown in Figure 4. The shape of the EUV spectra are the result of several factors, including the peak intensity of the laser at the time during the pulse when the emission is bright and phase-matched, the re-absorption of longer wavelengths by Argon gas, and the transmission of the Al filters, which were used to reject the fundamental laser and lower-order harmonics.

The HHG flux measured at the detector corresponds to a flux at the source of  $3.0 \times 10^{12}$  (+/-20%) photons/sec/harmonic for the 23<sup>rd</sup> harmonic at 30 nm ( $h\nu = 42$  eV). For 13.5 nm, the HHG flux measured at the detector corresponds to a flux at the source of  $3.0 \times 10^{10}$  (+/-20%) photons/sec/harmonic at 13.5 nm ( $h\nu = 92$  eV). This flux level is already being used for record spatial resolution imaging, achieving sub-wavelength spatial resolution of 12.5 nm at the technologically important 13.5 nm wavelength<sup>[2]</sup>.

In setting-up experiments that use EUV light, the difference between the HHG flux at the source and the flux deliverable to an experiment can be very substantial. Optical losses even in a highly-optimized beamline correspond to a throughput typically in the range of 0.1% - 10%. The exact value depends on the throughput of optics used to refocus or select a specific wavelength, as well

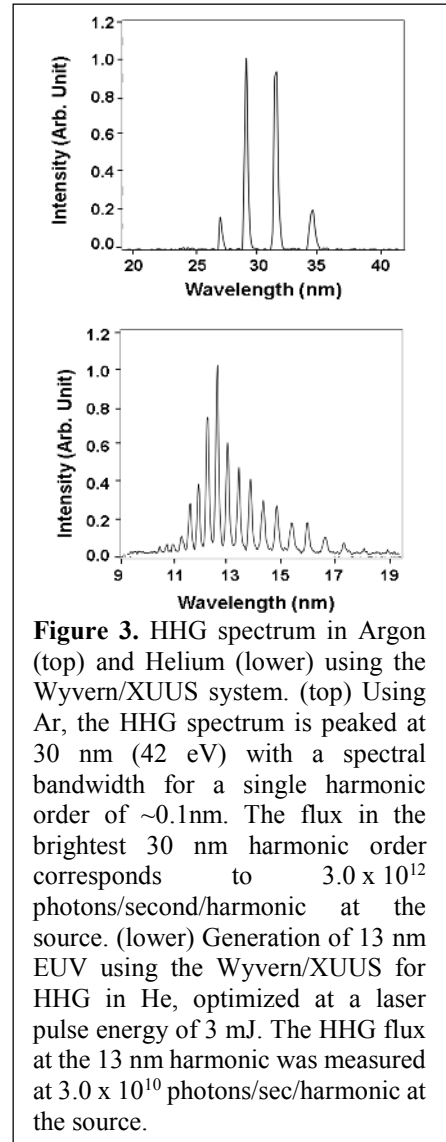


**Figure 3.** HHG spectrum in Argon (top) and Helium (lower) using the Wyvern/XUUS system. (top) Using Ar, the HHG spectrum is peaked at 30 nm (42 eV) with a spectral bandwidth for a single harmonic order of ~0.1nm. The flux in the brightest 30 nm harmonic order corresponds to  $3.0 \times 10^{12}$  photons/second/harmonic at the source. (lower) Generation of 13 nm EUV using the Wyvern/XUUS for HHG in He, optimized at a laser pulse energy of 3 mJ. The HHG flux at the 13 nm harmonic was measured at  $3.0 \times 10^{10}$  photons/sec/harmonic at the source.

at the throughput of the thin-film filters used block any visible/NIR light (necessary when using detectors such as CCD's that are sensitive to all wavelengths). *The specifics of the actual experimental application will determine the required throughput of the beam delivery system, and **must** be considered in any calculations of experimental throughput and feasibility.*

#### 4. Summary and Conclusions

These test results provide an example of the performance when the KMLabs Wyvern™ is used to drive the KMLabs XUUS<sub>4</sub>™. As the 1<sup>st</sup> commercial high-harmonic source, the XUUS<sub>4</sub>™ represents a revolutionary advance – bringing visible laser stability into the EUV region for the first time. This in turn is enabling revolutionary coherent microscopes based on tabletop HHG beams, that can very accurately extract nanoscale materials properties – including elemental/chemical, magnetic, electronic, elastic and transport properties. Moreover, by harnessing the exquisite coherence of HHG beams, the measurement limits for probing atomic, molecular, nano and materials systems can be dramatically advanced in both space and time, while significantly enhancing the sensitivity.

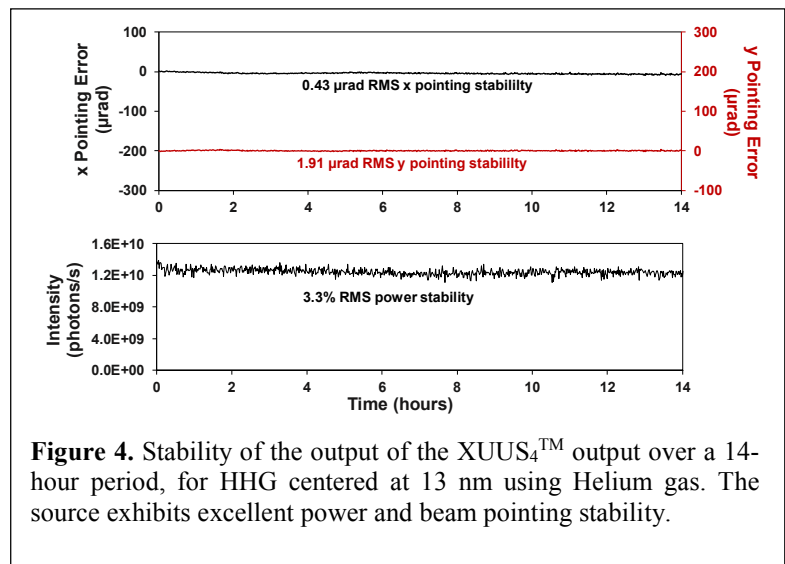


**Figure 4.** Stability of the output of the XUUS<sub>4</sub>™ output over a 14-hour period, for HHG centered at 13 nm using Helium gas. The source exhibits excellent power and beam pointing stability.

#### 5. References

1. A Rundquist, CG Durfee, ZH Chang, C Herne, S Backus, MM Murnane, and HC Kapteyn, "Phase-matched generation of coherent soft X-rays," *Science* **280**(5368), 1412-1415 (1998).
2. DF Gardner, M Tanksalvala, ER Shanblatt, X Zhang, BR Galloway, CL Porter, R Karl Jr, C Bevis, DE Adams, HC Kapteyn, MM Murnane, and GF Mancini, "Sub-wavelength coherent imaging of periodic samples using a 13.5 nm tabletop high-harmonic light source-," *Nature Photonics* **11**(4), 259-263 (2017). dx.doi.org/10.1038/nphoton.2017.33
3. RA Bartels, A Paul, H Green, HC Kapteyn, MM Murnane, S Backus, IP Christov, YW Liu, D Attwood, and C Jacobsen, "Generation of spatially coherent light at extreme ultraviolet wavelengths," *Science* **297**(5580), 376-378 (2002).
4. E Gagnon, P Ranitovic, A Paul, CL Cocke, MM Murnane, HC Kapteyn, and AS Sandhu, "Soft x-ray driven femtosecond molecular dynamics," *Science* **317**(5843), 1374-1378 (2007).
5. D Rudolf, C La-O-Vorakiat, M Battiato, R Adam, JM Shaw, E Turgut, P Maldonado, S Mathias, P Grychtol, HT Nembach, TJ Silva, M Aeschlimann, HC Kapteyn, MM Murnane, CM Schneider, and PM Oppeneer, "Ultrafast magnetization enhancement in metallic multilayers driven by superdiffusive spin current," *Nature Communications* **3**, 1037 (2012). dx.doi.org/10.1038/ncomms2029
6. S Mathias, C La-O-Vorakiat, P Grychtol, P Granitzka, E Turgut, JM Shaw, R Adam, HT Nembach, ME Siemens, S Eich, CM Schneider, TJ Silva, M Aeschlimann, MM Murnane, and HC Kapteyn, "Probing the timescale of the exchange interaction in a ferromagnetic alloy," *Proceedings of the National Academy of Sciences of the United States of America* **109**(13), 4792-4797 (2012). dx.doi.org/10.1073/pnas.1201371109
7. C Chen, ZS Tao, A Carr, P Matyba, T Szilvasi, S Emmerich, M Piecuch, M Keller, D Zusin, S Eich, M Rollinger, WJ Youa, S Mathias, U Thumm, M Mavrikakis, M Aeschlimann, PM Oppeneer, H Kapteyn, and M Murnane, "Distinguishing attosecond electron-electron scattering and screening in transition metals," *Proceedings of the National Academy of Sciences of the United States of America* **114**(27), E5300-E5307 (2017). dx.doi.org/10.1073/pnas.1706466114

8. KM Hoogeboom-Pot, E Turgut, JN Hernandez-Charpak, JM Shaw, HC Kapteyn, MM Murnane, and D Nardi, "Nondestructive Measurement of the Evolution of Layer-Specific Mechanical Properties in Sub-10 nm Bilayer Films," *Nano Letters* **16**(8), 4773-4778 (2016). [dx.doi.org/10.1021/acs.nanolett.6b00606](https://doi.org/10.1021/acs.nanolett.6b00606)
9. KM Hoogeboom-Pot, JN Hernandez-Charpak, X Gu, TD Frazer, EH Anderson, W Chao, RW Falcone, R Yang, MM Murnane, HC Kapteyn, and D Nardi, "A new regime of nanoscale thermal transport: Collective diffusion increases dissipation efficiency," *Proceedings of the National Academy of Sciences* **112**, 4846-4851 (2015). [dx.doi.org/10.1073/pnas.1503449112](https://doi.org/10.1073/pnas.1503449112)
10. S Eich, A Stange, AV Carr, J Urbancic, T Popmintchev, M Wiesenmayer, K Jansen, A Ruffing, S Jakobs, T Rohwer, S Hellmann, C Chen, P Matyba, L Kipp, K Rossnagel, M Bauer, MM Murnane, HC Kapteyn, S Mathias, and M Aeschlimann, "Time- and angle-resolved photoemission spectroscopy with optimized high-harmonic pulses using frequency-doubled Ti:Sapphire lasers," *Journal of Electron Spectroscopy and Related Phenomena* **195**, 231-236 (2014). [dx.doi.org/10.1016/j.elspec.2014.04.013](https://doi.org/10.1016/j.elspec.2014.04.013)
11. D Popmintchev, C Hernandez-Garcia, F Dollar, C Mancuso, JA Perez-Hernandez, M-C Chen, A Hankla, X Gao, B Shim, AL Gaeta, M Tarazkar, DA Romanov, RJ Levis, JA Gaffney, M Foord, SB Libby, A Jaron-Becker, A Becker, L Plaja, MM Murnane, HC Kapteyn, and T Popmintchev, "Ultraviolet surprise: Efficient soft x-ray high-harmonic generation in multiply ionized plasmas," *Science* **350**(6265), 1225-1231 (2015).
12. T Popmintchev, M-C Chen, D Popmintchev, P Arpin, S Brown, S Ališauskas, G Andriukaitis, T Balčiūnas, OD Mücke, A Pugzlys, A Baltuška, B Shim, SE Schrauth, A Gaeta, C Hernández-García, L Plaja, A Becker, A Jaron-Becker, MM Murnane, and HC Kapteyn, "Bright Coherent Ultrahigh Harmonics in the keV X-ray Regime from Mid-Infrared Femtosecond Lasers," *Science* **336**(6086), 1287-1291 (2012). [dx.doi.org/10.1126/science.1218497](https://doi.org/10.1126/science.1218497)
13. P Tengdin, W You, C Chen, X Shi, D Zusin, Y Zhang, C Gentry, A Blonsky, M Keller, P Oppeneer, H Kapteyn, Z Tao, and M Murnane, "Critical Behavior within 20fs Drives the Out-of-Equilibrium Laser-induced Magnetic Phase Transition in Nickel," *Science Advances* **in press** (2018).
14. D Popmintchev, B Galloway, MC Chen, F Dolar, C Mancuso, L Miaja-Avila, G O'Neil, J Shaw, G Fan, S Ališauskas, G Andriukaitis, T Balčiūnas, O Mücke, A Pugzlys, A Baltuška, H Kapteyn, T Popmintchev, and M Murnane, "Near and extended edge X-ray absorption fine structure spectroscopy using ultrafast coherent high harmonic supercontinua," *Physical Review Letters* **in press** (2018). [https://journals.aps.org/prl/accepted/de076Y00Tba19c7cb0db67b1e5451d70170ec08b0\(2018\)](https://journals.aps.org/prl/accepted/de076Y00Tba19c7cb0db67b1e5451d70170ec08b0(2018)).
15. ZS Tao, C Chen, T Szilvasi, M Keller, M Mavrikakis, H Kapteyn, and M Murnane, "Direct time-domain observation of attosecond final-state lifetimes in photoemission from solids," *Science* **353**(6294), 62-67 (2016). [dx.doi.org/10.1126/science.aaf6793](https://doi.org/10.1126/science.aaf6793)
16. CG Durfee III, A Rundquist, HC Kapteyn, and MM Murnane, "Guided wave methods and apparatus for nonlinear frequency generation," US Patent #6,151,155 (2000).
17. T Popmintchev, D Popmintchev, MM Murnane, and H Kapteyn, "Method for phase-matched generation of coherent VUV, EUV, and x-ray light using VUV-UV-VIS lasers," US Patent #61/873,794 (Notice of Allowance, 2015).
18. TV Popmintchev, DV Popmintchev, MM Murnane, and HC Kapteyn, "Generation of VUV, EUV, and X-ray Light Using VUV-UV-VIS Lasers," (Google Patents, 2017).
19. KMLabs, "XUUS™ Coherent EUV and Soft X-Ray Source" (2017), retrieved 11/12/2017, <https://kmlabs.com/product/xuus/>.

**Appendix A: EUV flux measurement methodology**

To accurately measure HHG flux, KMLabs used the beamline configuration as shown in Figure 5. There are many possible pitfalls in the accurate measurement of HHG flux-- primary among them is to block *all* background light from impinging on the detector, both at the fundamental driving laser wavelength of 800 nm, and at harmonic wavelengths that are within the detection range of the detector, but outside range of

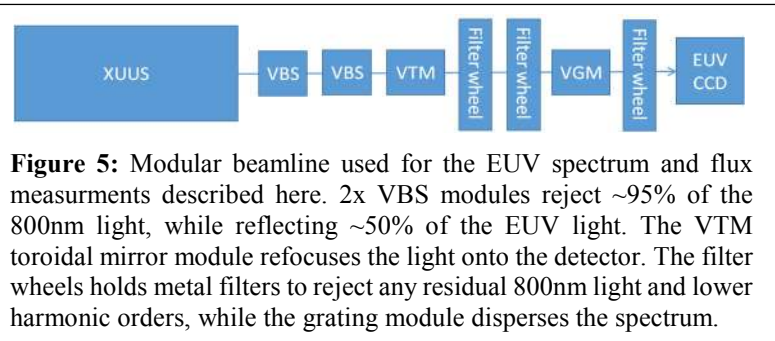


**Figure 5:** Modular beamline used for the EUV spectrum and flux measurements described here. 2x VBS modules reject ~95% of the 800nm light, while reflecting ~50% of the EUV light. The VTM toroidal mirror module refocuses the light onto the detector. The filter wheels holds metal filters to reject any residual 800nm light and lower harmonic orders, while the grating module disperses the spectrum.

Element	Throughput at 35 nm
VBS (2X), IR EUV beam separator module, to absorb 800 nm while reflecting EUV.	~70% each
Aluminum filters (2X), 1000 nm and 200 nm thick, to block 800 nm light as well as lower harmonic orders.	1.8% (1000 nm) 20% (200 nm)
A toroidal refocusing mirror	~70%
Diffraction grating (+1 order)	~16%
<b>Total beamline throughput</b>	0.02%
<b>Total beamline throughput without metal filters</b>	5.5%

**Table 3:** Beamline configuration and throughput for measurements of near EUV spectrum around 35 nm. Beamline throughput w/o metal filters is also estimated here as many experiments are not IR sensitive such as photoemission microscopy and spectroscopy.

wavelengths that are spectrally resolved. KMLabs has developed rigorous procedures that protect against false measurements. In the most rigorous process, the aggregate flux in an HHG beam is measured using a NIST-calibrated photodiode, with the spectrum subsequently dispersed onto a CCD to allow for the flux per harmonic order to be determined.

In this set of measurements, the CCD detector was cross-calibrated at KMLabs with the NIST-calibrated diode, with flux measurements determined using the CCD. Different spectral regions are calibrated using slightly different beamline configurations. For example, in the spectrum of Figure 3, the spectrum from 30-50 nm is isolated using the configuration as outlined in Table 3.

Two filters are used to avoid any 800 nm leakage through small pinholes that are inevitably present in any thin metal filter. Furthermore, since the throughput of these filters decreases with time due to oxidation, a series of three filters is employed in-line. Any two of these is sufficient to block out-of-band radiation, allowing the aggregate transmission of each filter over the spectral region of interest to be accurately measured. The dispersed spectrum is characterized with the CCD, with the flux in a single spectral peak estimated by the integrated counts measured on this detector, previously cross-referenced to the

flux measured using a NIST-calibrated diode. A flux at the source can then be backed-out taking into account the beamline efficiency.

For the 13.5 nm spectral measurement, the beamline parameters are given in Table 4.

Element	Throughput at 13.5 nm
VBS (2X)	~70% each
Zirconium filters (2X)	18% (200 nm) 16% (200 nm)
Toroidal refocusing mirror	~70%
Diffraction grating (+1 order)	~28%
<b>Total beamline throughput</b>	<b>0.28%</b>
<b>Total beamline throughput without metal filters</b>	<b>10%</b>

**Table 4:** Beamline configuration and throughput for measurements of near EUV spectrum around 13.5 nm. Beamline throughput w/o metal filters is also estimated here as many experiments are not IR sensitive, such as photoemission microscopy and spectroscopy.